Inorganica Chimica Acta, 208 (1993) 179–188

Tuning the spectroscopic and electrochemical properties of polypyridyl bridged mixed-metal trimetallic ruthenium(II), iridium(III) complexes: a spectroelectrochemical study

Jon S. Bridgewater, Lisa M. Vogler, Sharon M. Molnar and Karen J. Brewer*
Department of Chemistry, Virginia Polytechnic Institute and State University, Blacksburg, VA 24061-0212 (USA)

(Received November 25, 1992; revised February 11, 1993)

Abstract

A series of polypyridyl bridged trimetallic complexes of the type $\{[(bpy)_2Ru(BL)]_2IrCl_2\}^{5+}$ (where BL = 2,3-bis-2′-pyridylpyrazine (dpp), 2,3-bis-2′-pyridylquinoxaline (dpq) or 2,3-bis-2′-pyridylbenzoquinoxaline (dpb); bpy = 2,2′-bipyridine) have been prepared and their synthesis, characterization and spectroelectrochemical analysis are reported within. These complexes are of interest in that they contain two visible light absorbing centers covalently coupled to a known catalytically active central metal site. The trimetallic complexes show absorbances throughout the visible region of the spectrum and exhibit many electrochemical processes within the acetonitrile solvent window. All the systems studied possess a ruthenium based oxidative process as well as four bridging ligand based reductions, followed by iridium and bipyridine based reductive processes. The relative energy of the ruthenium based $d\pi$ highest-occupied molecular orbital (HOMO) remains constant for this series of trimetallic complexes. The energy of the lowest lying bridging ligand based π^* orbital, the lowest-unoccupied molecular orbital (LUMO), however, shifts to more positive potentials when dpq or dpb are substituted for dpp. This gives rise to a lowest energy absorption, $Ru(d\pi) \rightarrow BL(\pi^*)$ metal-to-ligand charge transfer (MLCT) transition, which can be tuned to lower energy as a function of bridging ligand from dpp to dpq to dpb. Through the synthetic variation of bridging ligand orbital energy and the use of spectroelectrochemical studies, it has been possible to elucidate the nature of the complex spectroscopy and electrochemistry of these supramolecular complexes. The dpp and dpq bridged systems emit in fluid solution at room temperature and their emission energies and lifetimes have been determined.

Introduction

In the field of photochemistry, there has been a great deal of interest in the excited state reactivity of complexes related to $[Ru(bpy)_3]^{2+}$ due to its long excited state lifetime in fluid solution and its ability to undergo excited state electron or energy transfer reactions [1]. The ability of $[Ru(bpy)_3]^{2+}$ to absorb visible light enables it to be considered for many solar energy conversion schemes, however, $[Ru(bpy)_3]^{2+}$ is inherently inefficient. One problem with $[Ru(bpy)_3]^{2+}$ is that the excited state electron or energy transfer is dependent upon a molecular collision before the excited $[Ru(bpy)_3]^{2+*}$ relaxes back to the ground state. Another problem with $[Ru(bpy)_3]^{2+}$ is that there is very little flexibility in the amount of energy or the number of electrons transferred by this photosensitizer.

Polymetallic complexes, on the other hand, have the ability to bring together all of the reaction partners so that a molecular collision is not needed to initiate the excited state electron or energy transfer reaction [2]. This would allow the polymetallic complex to have a much shorter lifetime than $[Ru(bpy)_3]^{2+}$, in which excited state electron or energy transfer will occur. Another advantage of polymetallic systems is their ability to store multiple electrons which could be eventually incorporated into solar energy conversion or electrocatalytic schemes [2–8].

With this in mind, a series of polypyridyl bridged mixed-metal trimetallic complexes of the general type $\{[(bpy)_2Ru(BL)]_2IrCl_2\}^{5+}$ (where BL = 2,3-bis-2′-pyridylpyrazine (dpp), 2,3-bis-2′-pyridylquinoxaline (dpq) or 2,3-bis-2′-pyridylbenzoquinoxaline (dpb); bpy = 2,2′-bipyridine) have been prepared and their electrochemical and photochemical properties investigated. A diagram of $\{[(bpy)_2Ru(dpp)]_2IrCl_2\}^{5+}$ is shown below.

---

*Author to whom correspondence should be addressed.

0020-1693/93/$6.00

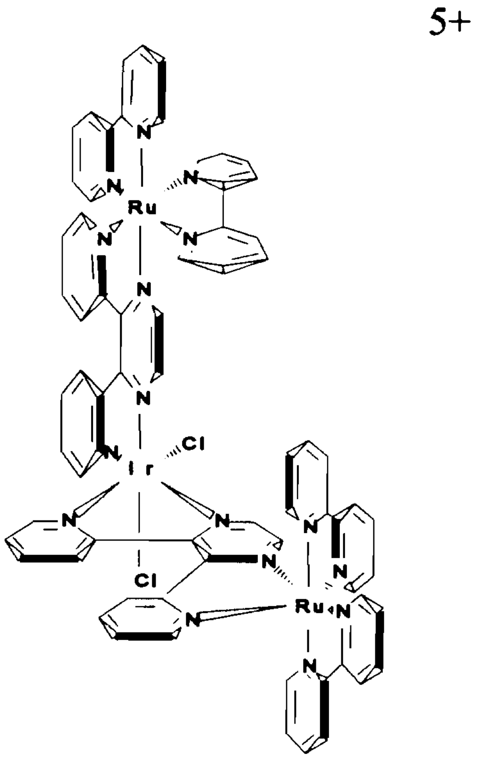

The series of bridging ligands used differs only by the addition of one and then two aromatic electron withdrawing groups bonded to the side of the pyrazine ring, see below [9].

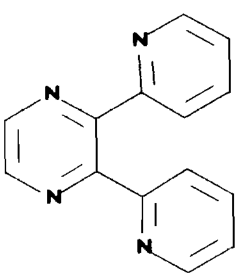

dpp

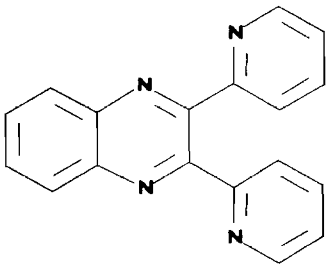

dpq

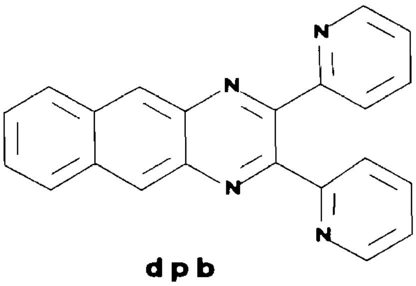

dpb

With the addition of each aromatic ring the bridging ligands become progressively easier to reduce.

Ruthenium complexes of the form $[Ru(bpy)_2(BL)]^{2+}$ have been shown to possess good light absorbing properties, resulting in the formation of a relatively long lived MLCT excited state [10, 11]. In addition, iridium monometallic complexes of the form $[Ir(BL)_2Cl_2]^+$ have been shown to be active catalysts for the reduction of carbon dioxide [12]. Therefore, each of these trimetallic complexes possesses two good light absorbing metal centers covalently coupled to a known catalytically active metal center. Visible light excitation of these systems results in population of an $Ru(d\pi) \rightarrow BL(\pi^*)$ MLCT excited state as illustrated below (LA = ruthenium light absorber, BL = bridging ligand, CAT = central iridium metal center).

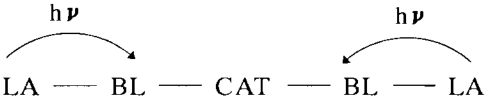

Since two light absorbers are present, these systems, as well as other complexes of this type, may have applications as photochemical molecular devices for electron collection [9a].

This particular series of polypyridyl bridged trimetallic complexes provides a unique opportunity to study perturbations introduced as a function of the bridging ligand in mixed-metal systems. This study indicates that both the energy of the MLCT excited states and the half-wave potentials of the first four reductions are dependent upon the nature of the polypyridyl bridging ligand used. The spectroscopic and electrochemical properties of these mixed-metal systems are reported herein.

Experimental

Materials

Materials were reagent grade and used without further purification. The iridium trichloride and ruthenium trichloride were supplied by Johnson Matthey through the precious metal loan program. The 2,3-bis(2′-pyridyl)pyrazine was purchased from Aldrich Chemical Company. The 2,3-bis(2′-pyridyl)quinoxaline was synthesized according to the methods of Goodwin and Lions by the reaction of *o*-phenylenediamine and 2,2′-pyridyl in ethanol [9a]. The 2,3-bis(2′-pyridyl)benzoquinoxaline was synthesized by a modification of the methods of Goodwin and Lions, substituting diaminonaphthalene for the *o*-phenylenediamine [9a–c]. The acetonitrile (Burdick and Jackson) used in the electrochemical and spectroscopic studies was of spectroquality, dried over activated alumina and stored over activated molecular sieves. The supporting electrolyte, tetrabutylammonium hexafluorophosphate (TBAH) was synthesized by the metathesis of tetrabutylammonium bromide (TBAB) with hexafluorophosphoric acid and recrystallized several times from hot ethanol. The electrolyte was dried in a vacuum oven and stored in a vacuum desiccator. The size exclusion resin, Sephadex LH-20, used was purchased from Pharmacia. The adsorption alumina used was purchased from Fisher Scientific. All other chemicals were Fisher Scientific reagent grade and were used without further purification.

Synthesis

$[Ru(bpy)_2Cl_2]$ [13], $[Ir(dpp)_2Cl_2]^+$ [12], $[Ir(dpq)_2Cl_2]^+$ [12] and $[Ir(dpb)_2Cl_2]^+$ [6] were prepared according to literature methods.

$\{[(bpy)_2Ru(dpp)]_2IrCl_2\}^{5+}$

Preparation of $\{[(bpy)_2Ru(dpp)]_2IrCl_2\}(PF_6)_5 \cdot EtOH$ was achieved by reacting $[Ir(dpp)_2Cl_2](PF_6)$ (0.288 g, 0.33 mmol) with $Ru(bpy)_2Cl_2$ (0.782 g, 1.0 mmol) in 50 ml of 2:1 (vol./vol.) ethanol/water. The solution was heated at reflux for *c*. 72 h. The resulting solution was removed from heat and a saturated solution of KPF_6 (50 ml) was added to induce precipitation of a purple–brown solid, which was separated by vacuum filtration. The product was washed with *c*. 30 ml of water to remove any excess KPF_6. The precipitate was then dissolved in a minimal amount of acetone (20 ml), this solution was filtered, and added with stirring to anhydrous diethyl ether (250 ml) to induce precipitation. The resulting precipitate was removed by vacuum filtration and was washed with *c*. 250 ml of anhydrous diethyl ether.

Purification of the product was achieved by size exclusion column chromatography. The precipitate was dissolved in a minimal amount of 2:1 (vol./vol.) ethanol/acetonitrile and filtered to remove any insoluble material. A 100-cm column was prepared using the same solvent mixture. The crude solution was loaded on the column and eluted with a 2:1 (vol./vol.) ethanol/acetonitrile mixture. The first band eluted was purple. Concentration of this solution by rotary evaporation followed by another chromatography step yielded the desired product. A typical yield for this product was 90%. Purity of the complex was established by chromatography of a small sample of the complex on a long size exclusion column, monitoring the electronic spectra of multiple fractions of the single band that formed as it eluted. All of the spectra were superimposable, indicating a pure sample. The size of the complex that was isolated was tested by the simultaneous loading of this new trimetallic complex and the previously reported bimetallic complex $\{[(bpy)_2Ru]_2(BL)\}^{4+}$ on a size exclusion column. The trimetallic complex eluted prior to the bimetallic system, consistent with its larger molecular size. *Anal.* Calc.: C, 36.1; H, 2.51; N, 9.62. Found: C, 36.0; H, 2.74; N, 9.65%.

$\{[(bpy)_2Ru(dpq)]_2IrCl_2\}^{5+}$

$\{[(bpy)_2Ru(dpq)]_2IrCl_2\}(PF_6)_5 \cdot EtOH$ was prepared as above substituting $[Ir(dpq)_2Cl_2](PF_6)$ (0.322 g, 0.33 mmol) for $[Ir(dpp)_2Cl_2](PF_6)$. A typical yield for the reaction was 85%. Purity was established as described for the analogous dpp complex. *Anal.* Calc.: C, 38.6; H, 2.57; N, 9.22. Found: C, 38.0; H, 2.65; N, 9.17%.

$\{[(bpy)_2Ru(dpb)]_2IrCl_2\}^{5+}$

$\{[(bpy)_2Ru(dpb)]_2IrCl_2\}(PF_6)_5 \cdot EtOH$ was prepared as above substituting $[Ir(dpb)_2Cl_2](PF_6)$ (0.355 g, 0.33 mmol) for $[Ir(dpp)_2Cl_2](PF_6)$. A typical yield for the reaction was 85%. Purity was established as described for the analogous dpp complex. *Anal.* Calc.: C, 40.8, H, 2.63; N, 8.86. Found: C, 41.0; H, 2.64; N, 8.77%.

Spectroscopy

Absorption spectra were recorded on a Hewlett Packard 8452 diode array spectrophotometer (resolution 2 nm) interfaced to a Hewlett Packard Vectra computer. Samples were prepared as acetonitrile solutions and measured at room temperature. Spectra were displayed on a Hewlett Packard ColorPro plotter.

Emission spectra were recorded as acetonitrile solutions on a Photon Technology Inc. MSIII spectrofluorometer which has a 150 W xenon arc lamp excitation source and a Hamamatsu R666S red-sensitive photomultiplier tube housed in a Products for Research thermoelectrically cooled single photon counting system (resolution 0.25 nm). Emission quantum yields were calculated relative to $[Os(bpy)_3]^{2+}$ ($\Phi = 0.00462$) in deoxygenated acetonitrile solution at room temperature [14].

Lifetime measurements

Emission lifetimes were determined using a Photon Technology Inc. PL 2300 nitrogen laser and a PL 201 continuously tunable dye laser (360–900 nm) excitation source. The luminescence was detected at a right-angle and passed through a monochromator for wavelength selection. The emission was detected by a Hamamatsu R666S red-sensitive photomultiplier tube contained in a Products for Research thermoelectrically cooled housing. The signal is digitized by a LeCroy 6880 fast digitizer and transferred to a computer for data handling (resolution 800 ps).

Electrochemistry

Cyclic voltammograms were recorded on a Bio-Analytical Systems 100A electrochemical analyzer equipped with a Houston Instruments DMP-40 digital plotter. The three electrodes were a glassy carbon disk working electrode, a platinum wire auxiliary electrode, and a silver/silver chloride gel reference electrode (0.286 V versus SHE). The solvent used was Burdick and Jackson high purity acetonitrile and the supporting electrolyte was 0.1 M TBAH (tetrabutylammonium hexafluorophosphate). The solutions were deoxygenated by bubbling with argon for 20 min prior to each scan, and blanketed with argon during the scan. The glassy carbon working electrode was manually cleaned prior to each scan. Half-wave potentials are reproducible to ±0.02 V.

Spectroelectrochemistry

Spectroelectrochemical measurements were performed utilizing a system that has been previously described [15]. All measurements were made on acetonitrile solutions that were *c.* 1×10^{-5} M in metal complex utilizing a platinum mesh working electrode.

Results

The series of polypyridyl bridged trimetallic complexes $\{[(bpy)_2Ru(dpp)]_2IrCl_2\}^{5+}$, $\{[(bpy)_2Ru(dpq)]_2IrCl_2\}^{5+}$ and $\{[(bpy)_2Ru(dpb)]_2IrCl_2\}^{5+}$ can be prepared under mild conditions from the monometallic components in extremely good yield using the synthetic methodology outlined below.

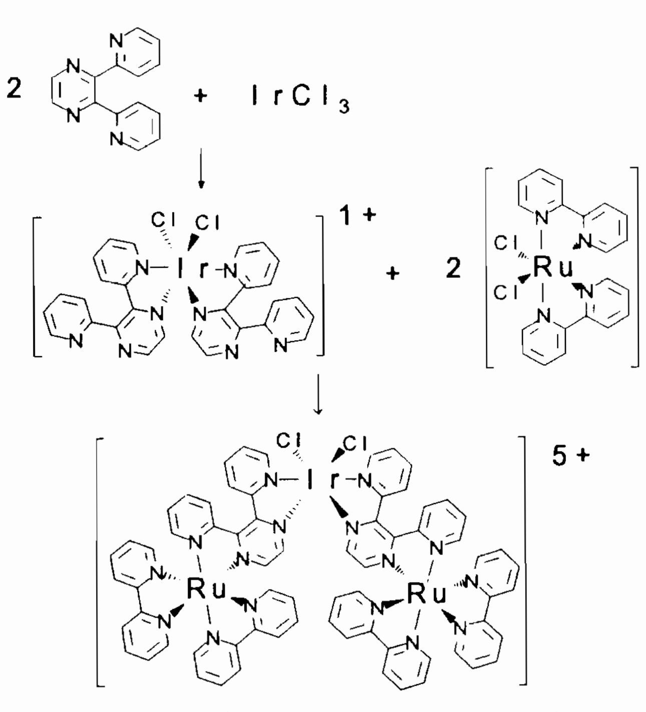

These mixed-metal systems contain two light absorbing metal centers, $Ru^{II}(bpy)_2(BL)$, covalently coupled through the bridging ligand to a catalytically active metal center, $Ir^{III}(BL)_2Cl_2$ [10–12].

The series of bridging ligands used in this study have been characterized in detail elsewhere [9]. The lowest energy absorption of the free ligands shifts to the red as the reduction potential shifts to more positive potential within this series from dpp to dpq to dpb. This behaviour is also exhibited by the monometallic ruthenium complexes of the type $[Ru(bpy)_2BL]^{2+}$ [4, 10, 11] as well as the iridium systems of the form $[Ir(BL)_2Cl_2]^+$ [12]. It is also of interest to note that the iridium based systems have bridging ligand reductions that occur at more positive potential than the $[Ru(bpy)_2(BL)]^{2+}$ complexes incorporating the same bridging ligands [1–12, 14].

The electronic spectral data for the title trimetallic mixed-metal complexes are shown in Fig. 1 and summarized in Table 1. Each spectrum has many overlapping bands throughout the UV and visible region of the spectrum. All complexes have very similar spectra in the UV (190–300 nm) with two intense peaks at *c.* 200 and 280 nm and a smaller set of shoulders at *c.* 250 nm. The visible region of the spectrum (300–800 nm) varies dramatically as a function of the bridging ligand used. Most notably, the lowest energy absorption shifts significantly to the red as the easier to reduce bridging ligands are substituted into the trimetallic framework.

Both the dpp and dpq bridged systems emit in fluid solution at room temperature. The emission maxima shifts to lower energy from 794 nm for $\{[(bpy)_2Ru(dpp)]_2IrCl_2\}^{5+}$ to 866 nm for $\{[(bpy)_2Ru(dpq)]_2IrCl_2\}^{5+}$. The emission lifetimes are 32 ns (fit to a single exponential decay) for the dpp and <5 ns for the dpq bridged systems.

The electrochemical data for the trimetallic complexes are summarized in Table 2 and a representative cyclic voltammogram is shown in Fig. 2. These systems exhibit one oxidative and seven reductive couples within the acetonitrile solvent window. The last three reductive waves overlap considerably, therefore no half-wave potentials are reported. The oxidative process occurs at the same potential for all of the trimetallics studied,

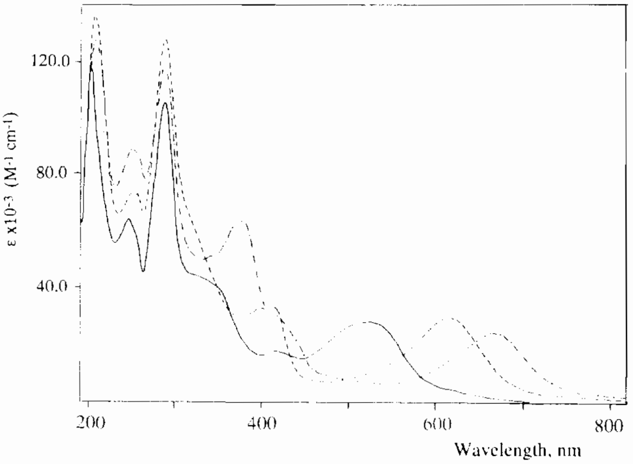

Fig. 1. Electronic spectra for a series of mixed-metal trimetallic complexes: ——, $\{[(bpy)_2Ru(dpp)]_2IrCl_2\}^{5+}$; – – –, $\{[(bpy)_2Ru(dpq)]_2IrCl_2\}^{5+}$; ·–·, $\{[(bpy)_2Ru(dpb)]_2IrCl_2\}^{5+}$.

TABLE 1. Electronic spectral data for a series of mixed-metal complexes incorporating polypyridyl bridging ligands

Complex	λ_{abs}(max.) (nm)	$\epsilon \times 10^{-3}$ (M^{-1} cm^{-1})	Assignment
$\{[(bpy)_2Ru(dpp)]_2IrCl_2\}^{5+}$	284	106	$n\rightarrow\pi^*$, $\pi\rightarrow\pi^*$ (bpy)
	326(sh)	43.5	Ru → bpy MLCT
	344(sh)	40.4	$\pi\rightarrow\pi^*$ (dpp)
	416	18.0	Ru → bpy MLCT
	522	27.9	Ru → dpp MLCT
$\{[(bpy)_2Ru(dpq)]_2IrCl_2\}^{5+}$	284	128	$n\rightarrow\pi^*$, $\pi\rightarrow\pi^*$ (bpy)
	324(sh)	58.2	Ru → bpy MLCT
	350(sh)	38.5	$\pi\rightarrow\pi^*$ (dpq)
	396	33.2	Ru → dpq MLCT
	414	33.6	Ru → bpy MLCT
	616	30.2	Ru → dpq MLCT
$\{[(bpy)_2Ru(dpb)]_2IrCl_2\}^{5+}$	284	118	$n\rightarrow\pi^*$, $\pi\rightarrow\pi^*$ (bpy)
	336(sh)	50.3	Ru → bpy MLCT
	374	63.5	$\pi\rightarrow\pi^*$ (dpb)
	416(sh)	30.7	Ru → bpy MLCT
	442(sh)	20.3	Ru → dpb MLCT
	666	24.8	Ru → dpb MLCT

TABLE 2. Cyclic voltammetric data for a series of mixed-metal trimetallic complexes incorporating polypyridyl bridging ligands

Complex	Oxidation	Reductions	
	$E_{1/2}$ (V)	$E_{1/2}$ (V)	$E_{1/2}$ (V)
$\{[(bpy)_2Ru(dpp)]_2IrCl_2\}^{5+}$	+1.56	−0.39 −1.06	−0.54 −1.22
$\{[(bpy)_2Ru(dpq)]_2IrCl_2\}^{5+}$	+1.56	−0.12 −0.90	−0.26 −1.22
$\{[(bpy)_2Ru(dpb)]_2IrCl_2\}^{5+}$	+1.56	+0.03 −0.71	−0.12 −0.98

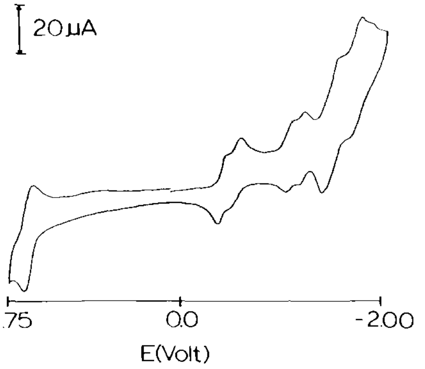

Fig. 2. Cyclic voltammogram for $\{[(bpy)_2Ru(dpp)]_2IrCl_2\}(PF_6)_5$ in acetonitrile.

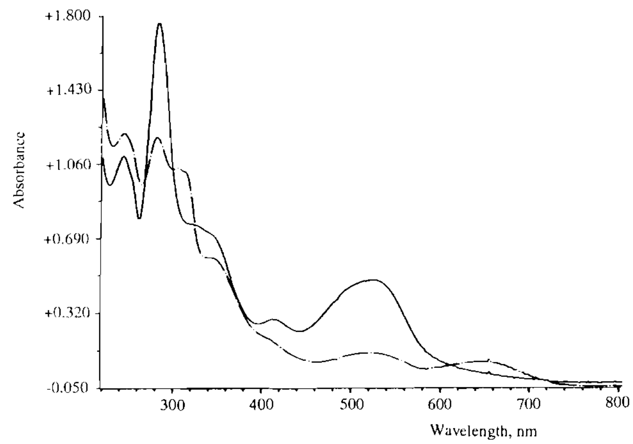

Fig. 3. Electronic spectra for $\{[(bpy)_2Ru(dpp)]_2IrCl_2\}^{n+}$: $n=5$ (——), 7 (·–·).

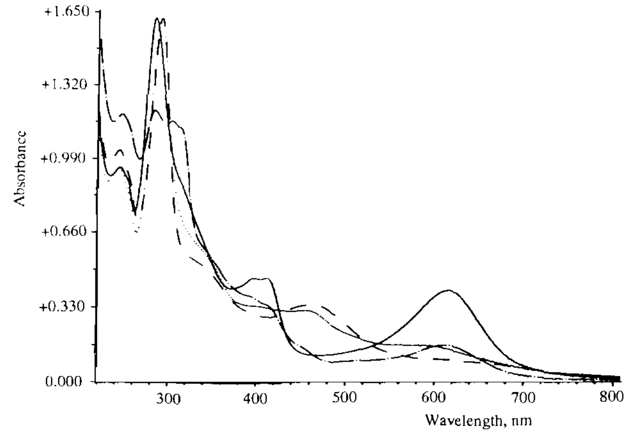

Fig. 4. Electronic spectra for $\{[(bpy)_2Ru(dpq)]_2IrCl_2\}^{n+}$: $n=5$ (——), 3 (·····), 1 (– – –), 7 (·–·).

while the first four reductive processes shift dramatically as a function of the bridging ligand incorporated.

The spectroelectrochemical results are shown in Figs. 3, 4 and 5. It was not possible to reversibly reduce the

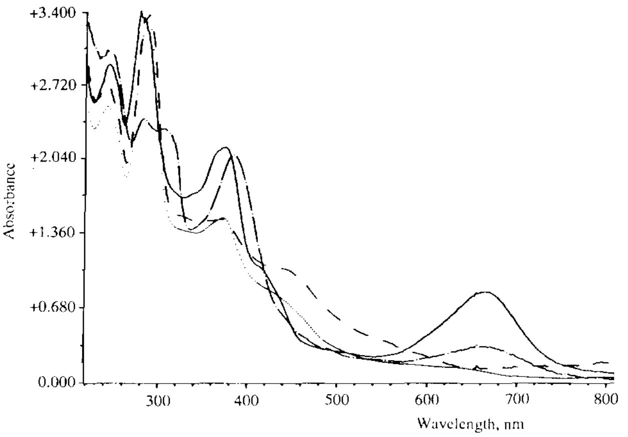

Fig. 5. Electronic spectra for $\{[(bpy)_2Ru(dpb)]_2IrCl_2\}^{n+}$: $n=5$ (——); 3 (·····), 1 (– – –), 7 (·–·).

dpp bridged system. Similar behavior was reported for the second reduction of $[(bpy)_2Ru]_2(dpp)^{4+}$ and is attributed to the pyridyl contribution to the LUMO of dpp resulting in bond cleavage [16a].

Discussion

One example of a homometallic ruthenium analog to these mixed-metal trimetallics appears in the literature, $\{[(bpy)_2Ru(dpp)]_2RuCl_2\}^{4+}$ [7b]. This system exhibits somewhat different behavior due primarily to an HOMO which is based on the central ruthenium center. As a result, this homometallic system is easier to oxidize than the iridium based system. In addition, the homometallic complex displays a lowest energy absorption that is red shifted relative to the mixed-metal complex, 618 versus 522 nm, respectively. This Ru→dpp MLCT absorption involves the central ruthenium in the homometallic complex and the terminal ruthenium centers in the mixed-metal complex. Finally, the homometallic system is not emissive at <880 nm under the conditions studied due to the nature and energy of the lowest lying excited state.

The lowest energy π^* orbital of the bridging ligand is stabilized as the electron withdrawing benzene rings are fused to the side of the pyrazine moiety, going from dpp to dpq to dpb [8, 9, 16]. Since the LUMO in these polymetallic complexes is bridging ligand based, this stabilization of the π^* orbital will dominate the trends seen in the metal complexes containing these bridging ligands. This makes possible the tuning of the spectroscopic and electrochemical properties of metal complexes as a function of the reduction potential of the bridging ligand used while maintaining a fairly constant coordination environment on the metal center [10, 11, 17–19].

Spectroscopy

The electronic spectra of the mixed-metal systems $\{[(bpy)_2Ru(BL)]_2IrCl_2\}^{5+}$, Fig. 1 and Table 1, consist of ligand localized $\pi\rightarrow\pi^*$ transitions in the UV and a series of MLCT bands in the visible. Ligand localized $\pi\rightarrow\pi^*$ transitions for both the bpy and the bridging ligand are expected. The bpy based $\pi\rightarrow\pi^*$ do not typically shift upon formation of a multimetallic system. However, bridging ligand based $\pi\rightarrow\pi^*$ transitions shift to lower energy upon formation of multimetallic systems. Due to the presence of four bipyridines per two bridging ligands in these multimetallic systems, bipyridine based $\pi\rightarrow\pi^*$ bands dominate the UV region of the spectrum. This gives rise to the similar band shapes in the 190–300 nm region of the spectrum for this series of trimetallic complexes. The difference in the ϵ values in this region can be attributed to the presence of bridging ligand based $\pi\rightarrow\pi^*$ transitions which add intensity to different regions of the spectrum dependent on the bridging ligand present.

The visible region of the spectrum should contain a series of MLCT bands. The lowest energy transition in each of these complexes is assigned to an $Ru(d\pi)\rightarrow BL(\pi^*)$ metal-to-bridging ligand charge transfer. This $Ru(d\pi)\rightarrow BL(\pi^*)$ transition is present in the ruthenium monometallic complexes, $[Ru(bpy)_2(BL)_2]^{2+}$ [10, 11], and shifts to lower energy upon formation of the bridged species. The trend observed is quite similar to that seen for the homometallic systems $\{[(bpy)_2Ru]_2(BL)\}^{4+}$ [8, 10, 11, 16]. A larger shift is observed for the trimetallic complexes and is attributed to an increased stabilization of the bridging ligand based π^* orbital due to higher positive charge on the iridium(III) metal center. This lowest energy band shifts to the red as the easier to reduce bridging ligands dpq and dpb are substituted for dpp, consistent with the $Ru(d\pi)\rightarrow BL(\pi^*)$ MLCT assignment. The relatively high extinction coefficients for these MLCT transitions are inconsistent with an iridium based process at this energy [12, 20].

The bridging ligands are coordinated to two electropositive metals in the trimetallic complexes. This results in a stabilization of the π^* orbitals of the bridging ligands. This stabilization gives rise to the observed shift in the lowest energy $Ru(d\pi)\rightarrow BL(\pi^*)$ MLCT transition of the trimetallics to a lower energy than the corresponding $[Ru(bpy)_2(BL)]^{2+}$ monometallic analogs. In addition, this stabilization will result in a shift of BL based $\pi\rightarrow\pi^*$ transitions. For this reason, these bridging ligand based transitions should reach into the visible (>300 nm). Shoulders seen in all the spectra from 300–400 nm could contain these $\pi\rightarrow\pi^*$ based transitions. The presence of a transition in all of the trimetallic spectra at c. 415 nm indicates that this peak is not dependent on the nature of the bridging ligand orbital and may represent the Ru(dπ)$\rightarrow$bpy(π^*) MLCT transition that is expected to occur in this region and at similar energy for all of these complexes [1, 8, 10, 11, 16]. A more detailed analysis of the spectroscopy follows in the spectroelectrochemical discussion.

The dpp and dpq bridged systems exhibit detectable emission in the visible following excitation of the Ru$\rightarrow$BL MLCT transition. The energy of this emission varies as a function of bridging ligand with the dpp bridged system emitting at higher energy than the analogous dpq complex. The dpb bridged system does not show an emission detectable on our system. This is most likely due to the expected low energy and shorter lifetime of this emission, which is beyond our detection capabilities. Both the dpp and dpq bridged complexes display a shorter excited state lifetime than the $[Ru(bpy)_2(BL)]^{2+}$ monometallic analogs. The magnitude of the lifetimes are consistent with a ruthenium based charge transfer excited state. The shortened lifetime, upon formation of the trimetallic species, indicates a more rapid decay of the ruthenium based MLCT excited state, facilitated by the introduction of the $Ir^{III}Cl_2(BL)Ru^{II}(bpy)_2$ fragment. The quantum yield for emission for the dpp bridged system at room temperature is 0.00012. This is significantly lower than $[Ru(bpy)_2(dpp)]^{2+}$ [10], indicating an enhancement in the radiationless decay efficiency of these supramolecular complexes. The dpq bridged system has a much lower emission intensity with a quantum yield $<10^{-6}$.

Electrochemistry

The cyclic voltammetry of these trimetallic complexes is expected to be complicated due to the presence of a large number of electroactive moieties, i.e. 2Ru, Ir, 4bpy and 2BL. The proposed electrochemical mechanism for the oxidative wave and the first four reductive waves of these systems is given below.

$$[(bpy)_2Ru^{(III)}(BL)Ir^{(III)}(BL)Ru^{(III)}(bpy)_2]^{7+}$$
$$+2e^- \downarrow\uparrow -2e^-$$
$$*\ [(bpy)_2Ru^{(II)}(BL)Ir^{(III)}(BL)Ru^{(II)}(bpy)_2]^{5+}$$
$$+e^- \downarrow\uparrow -e^-$$
$$[(bpy)_2Ru^{(II)}(BL^-)Ir^{(III)}(BL)Ru^{(II)}(bpy)_2]^{4+}$$
$$+e^- \downarrow\uparrow -e^-$$
$$[(bpy)_2Ru^{(II)}(BL^-)Ir^{(III)}(BL^-)Ru^{(II)}(bpy)_2]^{3+}$$
$$+e^- \downarrow\uparrow -e^-$$
$$[(bpy)_2Ru^{(II)}(BL^{2-})Ir^{(III)}(BL^-)Ru^{(II)}(bpy)_2]^{2+}$$
$$+e^- \downarrow\uparrow -e^-$$
$$[(bpy)_2Ru^{(II)}(BL^{2-})Ir^{(III)}(BL^{2-})Ru^{(II)}(bpy)_2]^{1+}$$

The * indicates the oxidation state of the system which is synthesized, prior to any electrochemical oxidations or reductions. The only oxidative process seen in the solvent window represents the simultaneous oxidation of the Ru(II) centers to Ru(III). The increased peak current relative to the other waves is consistent with this assignment. The position of this oxidative wave is in agreement with a ruthenium based process and inconsistent with an iridium based oxidation [10–12, 17, 18, 21]. The increased ΔE_p ($\Delta E_p = E_p{}^a - E_p{}^c$) for this wave ($>100$ mV) indicates that it may in fact result from two closely spaced one-electron oxidations. These two equivalent metal centers exhibit one visible oxidative wave indicating that they are not significantly electronically coupled through the bridging ligand–iridium–bridging ligand framework. The ruthenium based oxidation shifts to a more positive potential as the $[Ru(bpy)_2(BL)]^{2+}$ moieties are incorporated into the trimetallic framework. This is consistent with the electron withdrawing effect of the additional positive metal centers present in the trimetallic complex. The half-wave potential of this ruthenium based oxidation is *independent* of the bridging ligand used, indicating that the substitution of easier to reduce bridging ligands into this trimetallic framework has no effect on the relative energy of the ruthenium based dπ HOMO. No oxidation is observed for the iridium metal center. This is in agreement with the electrochemical behaviour of the $[Ir(BL)_2Cl_2]^+$ monometallic analogs [12].

It has been noted by several authors that the BL π^* orbitals are stabilized upon bridging between two electropositive metals [4, 6, 8, 10, 11, 16, 17, 19, 21]. The bridging ligand's π^* orbitals in these complexes are highly stabilized as evidenced by two sets of bridging ligand based reductions prior to other reductive processes. This is consistent with electrochemical studies on $\{[(bpy)_2Ru]_2(BL)\}^{4+}$ systems where two bridging ligand based reductions occur prior to bpy based reductions [8, 10, 11, 16, 17, 19]. In these trimetallic systems, two bridging ligands are present and each is reduced separately, since the two equivalent bridging ligands are electronically coupled through the iridium metal center. The separation between the two bridging ligand based reductions in each pair of reductive processes is indicative of the electronic coupling of the two equivalent bridging ligands. For the first set of reductions, which represent the two sequential BL/BL$^-$ couples, a similar process can be observed in the monometallic analogs, $[Ir(BL)_2Cl_2]^+$. All of the trimetallic complexes exhibit similar $\Delta E_{1/2}$ ($\Delta E_{1/2} = E_{1/2}{}^{red}(1) - E_{1/2}{}^{red}(2)$), with values for the first set of bridging ligand based reductions ranging from 0.14 to 0.15 V. These values are somewhat smaller than for the analogous iridium monometallic complexes. This decreased coupling of the bridging ligands in the trimetallic complexes could be attributed to a polarization of this π^* orbital away from the iridium metal center by the coordination of the ruthenium metal center to the remote nitrogens on the bridging ligands giving rise to decreased coupling of the bridging ligands through the iridium metal center. The $\Delta E_{1/2}$ values for the second set of bridging ligand based reductions, corresponding to the two sequential BL^-/BL^{2-} processes, are substantially different for dpp (0.16 V) than for dpq (0.32 V) or dpb (0.27 V). The two-electron reduced form of dpp shows a much lower degree of coupling to the second bridging ligand coordinated to the central metal center than does dpq or dpb. Wertz and co-workers [16a] have shown that the LUMO occupied in the one-electron reduced form of $\{[(bpy)_2Ru]_2(dpp)\}^{4+}$ is spread over the pyridine and pyrazine portion of the ligand while the analogous dpq system appears to be localized on the quinoxaline portion of the ligand. When two electrons are added to bridging ligand based orbitals in these trimetallic complexes, substantially different bridging ligand to bridging ligand coupling is observed. This could result from the increased negative charge density being polarized away from the iridium metal center, towards the remote pyridine ring in the dpp bridged trimetallic. This may not be possible in the analogous dpq and dpb bridged systems where the orbital may reside primarily on the quinoxaline and benzoquinoxaline portion of the ligand. Both sets of bridging ligand based reductions shift to more positive potentials as the bridging ligand is varied from dpp to dpq to dpb. Therefore, the relative energy of the bridging ligand based LUMO changes dramatically within this series of complexes.

Additional reductive processes in these systems are expected to involve the two-electron reduction of the iridium metal center from Ir(III) to Ir(I) as well as two sets of bpy based reductions [12, 16, 17, 19, 21]. The iridium based reduction should be irreversible due to the tendency of the electrogenerated Ir(I) metal center to adopt a four-coordinate geometry by loss of two chloride ligands [12, 21]. In addition, two sequential two-electron reductive processes are expected, corresponding to the reduction of the first and then second bipyridine coordinated to the two ruthenium centers [8, 10, 11, 16–18]. These processes can be observed for all of the trimetallic complexes, however, considerable overlap of reductive waves is encountered in this region.

Spectroelectrochemistry

It was possible to generate the two-electron oxidized form of all of the systems as well as the two- and four-electron reduced form of the dpq and dpb bridged complexes. The electronic spectra of these electrogenerated complexes is shown in Figs. 3, 4 and 5. It was not possible to reversibly reduce the dpp bridged system. This result is consistent with results obtained on other dpp containing complexes [8, 10, 11, 16]. Wertz and co-workers explained this result in terms of a pyridyl contribution to the dpp LUMO, absent in dpq [16a]. Interestingly, the fragmentation of our trimetallic system appears to occur through rupture of the dpp–iridium bonds, since the spectrum of the decomposed system is consistent with $[Ru(bpy)_2(dpp)]^{2+}$ formation.

All of the trimetallic systems exhibit a loss of the lowest lying absorption upon generation of the two-electron oxidized form, consistent with a ruthenium based oxidation giving rise to loss of a Ru based MLCT. Both the two- and four-electron reductions give spectral changes consistent with a bridging ligand based process and inconsistent with a bipyridine based reduction [14, 16a]. Close examination of these results has yielded the following spectroscopic assignments.

$\{[(bpy)_2Ru(dpb)]_2IrCl_2\}^{5+}$ exhibits absorption maxima at 284, 336, 374, 416(sh), 442(sh) and 666 nm. The lowest energy band at 666 nm is lost upon two-electron oxidation or two- or four-electron reduction. This observation is consistent with an $Ru(d\pi) \rightarrow dpb(\pi^*)$ MLCT assignment. The two higher energy shoulders at 416 and 442 nm exhibit different behavior. Upon oxidation of the two ruthenium centers, both shoulders are lost. This is consistent with an MLCT assignment. Upon either two- or four-electron reduction, one shoulder is lost and the other shifts to lower energy. Since the first four reductions are dpb based, the shoulder at 442 nm which is lost represents a higher energy Ru → dpb MLCT. A shift to lower energy of a bpy based MLCT upon reduction of the bridging ligand has been observed for $[(bpy)_2Ru]_2(BL)^{4+}$ complexes [14, 16a]. Therefore, the shoulder at 416 nm which shifts to lower energy upon dpb reduction is assigned as an Ru → bpy MLCT. The shift to lower energy of this transition can be attributed to a destabilization of the ruthenium based $d\pi$ orbitals due to the decreased π acceptor ability of the reduced dpb ligand.

The intense band at 374 nm in the parent complex diminishes in intensity upon two- or four-electron reduction and shifts to lower energy in the two-electron oxidized species. This behaviour is consistent with a dpb based $\pi \rightarrow \pi^*$ transition. The shift to lower energy of this absorption upon oxidation of the ruthenium centers is consistent with a stabilization of the π^* orbital facilitated by interaction with the more positive ruthenium(III) centers. A small shoulder which is present at 336 nm appears to be lost upon oxidation of the ruthenium centers. This shoulder is also present in the dpq and dpp bridged complexes and may represent a higher energy Ru → bpy MLCT. The very intense transition at 284 nm is relatively unchanged by two- or four-electron reduction but splits into two components upon two-electron oxidation to generate the ruthenium(III) species. This behaviour is observed for the dpp, dpq and dpb bridged complexes. It appears that this band represents two overlapping transitions with one shifting to lower energy upon oxidation and the other remaining relatively unchanged. Peaks in this region have been attributed to overlapping $n \rightarrow \pi^*$, $\pi \rightarrow \pi^*$ transitions based on bpy [8, 10, 11, 12a, 16, 22]. Oxidation of the ruthenium centers should result in a stabilization of the π^* orbitals based on bpy due to the decreased π backbonding ability of the ruthenium(III) center. Metal oxidation would not be expected to have a significant effect on the energy of the π orbitals on bpy. Thus, as observed for the dpb based $\pi \rightarrow \pi^*$ transitions, bpy based $\pi \rightarrow \pi^*$ transitions should shift to lower energy upon oxidation of the ruthenium. The non-bonding bpy orbitals should be stabilized by oxidation of the ruthenium center due to the increased σ acceptor ability of the metal center. Since both the n and π^* orbitals based on bpy should be stabilized upon ruthenium oxidation, the energy gap between these two and thus the absorption maxima should remain relatively constant as the ruthenium centers are oxidized. Hence the absorption at 284 nm in the parent complex is assigned as overlapping $n \rightarrow \pi^*$, $\pi \rightarrow \pi^*$ transitions based on bpy.

Similar effects are observed upon oxidation or reduction of the dpq bridged system. Comparison of the electronic spectra of the synthesized and electrogenerated oxidation states has resulted in the assignments presented in Table 1. The absorption maxima at 284, 324 and 414 nm exhibit the same behaviour as seen in the dpb bridged complex, consistent with their assignments as overlapping $n \rightarrow \pi^*$ and $\pi \rightarrow \pi^*$, Ru → bpy MLCT and Ru → bpy MLCT, respectively. The shoulder at 350 nm in the parent complex is absent in the $4e^-$ reduced form and shifts to lower energy in the $2e^-$ oxidized form. This behaviour as well as the energy and ϵ of this transition are consistent with a $\pi \rightarrow \pi^*$ based on dpq. The peaks at 396 and 616 nm are lost upon $2e^-$ oxidation or $4e^-$ reduction, consistent with their Ru → dpq MLCT assignment.

Oxidation of the dpp bridged complex gave rise to a splitting of the band at 284 nm as seen in the dpq and dpb complexes. In addition, loss of the transitions at 326, 416 and 522 nm is observed. This along with their relative energies as compared to the dpq and dpb complexes yields their assignments as bpy based, bpy based and dpp based MLCT transitions involving the ruthenium. Oxidation of the dpp bridged complex results in the observation of a new transition centered around 650 nm. This new peak is also seen in the ruthenium(III),M(III) forms of complexes of the type $\{[(bpy)_2Ru(dpp)]_2MCl_2\}^{n+}$, M = Rh or Os [23] and may represent a dpp → Ru LMCT which appears upon oxidation of the ruthenium metal center.

Conclusions

Through the variation of the bridging ligand in complexes of the type $\{[(bpy)_2Ru(BL)]_2IrCl_2\}^{5+}$, it has been possible to tune the ground and excited state properties of these mixed-metal systems. In addition, this synthetic modification and spectroelectrochemical studies have illustrated the power of these techniques to yield considerable insight into the nature of the complex spectroscopic and electrochemical properties of these supramolecular complexes. For all three of the complexes studied, the relative energy of the ruthenium based HOMO remains unchanged while the relative energy of the bridging ligand based LUMO varies dramatically. This gives rise to a series of similar complexes in which properties directly related to the π^* LUMO energy vary while those associated with other parts of the molecule remain essentially constant. This is manifested in the similar UV and varied visible spectra as well as the constant oxidation potential and varied first four reduction potentials for this series of complexes. Due to the covalent coupling of two good light absorbing metals, i.e. the two ruthenium centers, to a known catalytically active metal center, i.e. the iridium center, these systems may have applications in photocatalysis [20, 23]. All of these trimetallic complexes have a lowest lying excited state that is $Ru(d\pi) \rightarrow BL(\pi^*)$ in nature. Thus, photoexcitation of these molecules leads to transfer of an electron from the ruthenium light absorbing metal, to the bridging ligand, in the direction of the central catalytic metal center, iridium. Studies are currently in progress to determine both the electrocatalytic and photocatalytic behaviour of these molecules [23].

Acknowledgements

We thank Johnson Matthey for the loan of the iridium and ruthenium metals used in this study. This investigation was supported in part by funds provided by Virginia Polytechnic Institute and State University, Washington State University and the National Science Foundation (CHE 9108374). Acknowledgement is made to the Donors of The Petroleum Research Fund, administered by the American Chemical Society, for partial support of this research.

References

1 (a) G. Navon and N. Suton, *Inorg. Chem., 13* (1974) 2159; (b) H. D. Gafney and A. W. Adamson, *J. Am. Chem. Soc., 94* (1972) 8238; (c) C.-T. Lin, W. Bottcher, M. Chou, C.

Creutz and N. Sutin, *J. Am. Chem. Soc., 98* (1976) 6536; (d) H. D. Gafney and A. W. Adamson, *J. Am. Chem. Soc., 94* (1972) 8238; (e) C. R. Bock, T. J. Meyer and D. G. Whitten, *J. Am. Chem. Soc., 96* (1974) 4710; (f) C. R. Bock, J. A. Connor, A. R. Gutierrez, T. J. Meyer, D. G. Whitten, B. P. Sullivan and J. K. Nagle, *J. Am. Chem. Soc., 101* (1979) 4815; (g) N. Sutin and C. Creutz, *Adv. Chem. Ser. No. 168,* (1978) 1; (h) T. J. Meyer, *Acc. Chem. Res., 11* (1978) 94; (i) N. Sabbatini and V. Balzani, *J. Am. Chem. Soc., 94* (1972) 7587; (j) J. N. Demas and A. W. Adamson, *J. Am. Chem. Soc., 93* (1972) 1800; (k) N. A. P. Kane-Maguire and C. H. Langford, *J. Am. Chem. Soc., 94* (1972) 2121; (l) V. Balzani, L. Moggi, M. F. Manfrin, F. Bolletta and G. A. Laurence, *Coord. Chem. Rev., 15* (1975) 321; (m) F. H. Burstall, *J. Chem. Soc.,* (1936) 173.

2 (a) V. Balzani, *Supramolecular Photochemistry,* NATO ASI Series 214, Reidel, Dordrecht, 1987, p. 135; (b) V. Balzani and L. Moggi, *Coord. Chem. Rev., 97* (1990) 313; (c) T. J. Meyer, *Acc. Chem. Res., 22* (1989) 163; (d) V. Balzani, *J. Photochem. Photobiol., 51* (1990) 55; (e) F. Scandola, C. A. Bignozzi, C. Chiorboli, M. T. Indelli and M. A. Rampi, *Coord. Chem. Rev., 97* (1990) 299; (f) J.-M. Lehn, *Angew. Chem., 27* (1988) 89; (g) J. D. Petersen, W. R. Murphy, R. Sahai, K. J. Brewer and R. R. Ruminski, *Coord. Chem. Rev., 64* (1985) 261; (h) Y. Lei, T. Buranda and J. F. Endicott, *J. Am. Chem. Soc., 112* (1990) 8820; (i) K. S. Schanze, G. A. Neyhart and T. J. Meyer, *J. Phys. Chem., 90* (1986) 2182.

3 R. R. Ruminski, J. Kiplinger, T. Cockroft and C. Chase, *Inorg. Chem., 28* (1989) 370.

4 F. Barigelletti, L. De Cola, V. Balzani, R. Hage, J. G. Haasnoot, J. Reedijk and J. G. Vos, *Inorg. Chem., 28* (1989) 4344.

5 M. Hunziker and A. Ludi, *J. Am. Chem. Soc., 99* (1977) 7370.

6 D. P. Rillema, R. W. Callahan and K. B. Mack, *Inorg. Chem., 21* (1982) 2589.

7 (a) G. Denti, S. Campagna, L. Sabatino, S. Serroni, M. Ciano and V. Balzani, *Inorg. Chim. Acta, 176* (1990) 175; (b) G. Denti, S. Campagna, S. Serroni, M. Ciano and V. Balzani, *J. Am. Chem. Soc., 114* (1992) 2944.

8 W. R. Murphy, K. J. Brewer, G. Gettliffe and J. D. Petersen, *Inorg. Chem., 28* (1989) 81.

9 (a) H. A. Goodwin and F. Lions, *J. Am. Chem. Soc., 81* (1959) 6415; (b) A. Escuer, T. Comas, J. Ribas, R. Vicente, X. Solans, C. Zanchini and D. Gatteschi, *Inorg. Chim. Acta, 162* (1989) 97; (c) N. P. Buu-Hoi and G. Saint-Ruf, *J. Chem. Soc.,* (1961) 2257; (d) F. C. Trusell and W. F. McKenzie, *Anal. Chim. Acta, 40* (1968) 350; (e) W. I. Stephen and P. C. Uden, *Anal. Chim. Acta, 39* (1967) 357.

10 C. H. Braunstein, A. D. Baker, T. C. Strekas and H. D. Gafney, *Inorg. Chem., 23* (1984) 857.

11 (a) D. P. Rillema and K. B. Mack, *Inorg. Chem., 21* (1982) 3849; (b) D. L. Carlson and W. R. Murphy, *Inorg. Chim. Acta, 181* (1991) 61.

12 S. R. Rasmussen, M. M. Richter, E. Yi, H. Place and K. J. Brewer, *Inorg. Chem., 29* (1990) 3926.

13 B. P. Sullivan, D. J. Salmon and T. J. Meyer, *Inorg. Chem., 17* (1978) 3334.

14 J. V. Caspar, E. M. Kober, B. P. Sullivan and T. J. Meyer, *J. Am. Chem. Soc., 104* (1982) 630.

15 K. J. Brewer, R. S. Lumpkin, J. W. Otvos, L. O. Spreer and M. Calvin, *Inorg. Chem., 28* (1989) 4446.

16 (a) J. B. Cooper, D. B. MacQueen, J. D. Petersen and D. W. Wertz, *Inorg. Chem., 29* (1990) 3701; (b) W. R. Murphy, personal communication; (c) J. D. Petersen, *Supramolecular Photochemistry,* NATO ASI Series 214, Reidel, Dordrecht, 1987, p. 135; (d) M. M. Richter and K. J. Brewer, *Inorg. Chim. Acta, 180* (1991) 125; (e) *Inorg. Chem., 31* (1992) 1594; (f) *Inorg. Chem.,* (1993) in press.

17 Y. Fuchs, S. Lofters, T. Dieter, W. Shi, R. Morgan, T. C. Strekas, H. D. Gafney and A. D. Baker, *J. Am. Chem. Soc., 109* (1987) 2691.

18 R. M. Berger, *Inorg. Chem., 29* (1990) 1920.

19 (a) J. A. Baiano, D. L. Carlson, G. M. Wolosh, D. E. DeJesus, C. F. Knowles, E. G. Szabo and W. R. Murphy, *Inorg. Chem., 29* (1990) 2327; (b) G. Denti, S. Campagna, L. Sabatino, S. Scolastica, M. Ciano and V. Balzani, *Inorg. Chem., 29* (1990) 4750; (c) R. Sahai, L. Morgan and D. P. Rillema, *Inorg. Chem., 27* (1988) 3495; (d) N. E. Katz, C. Creutz and N. Sutin, *Inorg. Chem., 27* (1988) 1687; (e) K. Kalyanasundaram and Md. K. Nazeeruddin, *Chem. Phys. Lett., 158* (1989) 45; (f) G. Tapolsky, R. Duesing and T. J. Meyer, *Inorg. Chem., 29* (1990) 2285; (g) W. Kaim and S. Kohlmann, *Inorg. Chem., 29* (1990) 2909; (h) D. P. Rillema, D. G. Taghdiri, D. S. Jones, C. D. Keller, L. A. Worl, T. J. Meyer and H. A. Levy, *Inorg. Chem., 26* (1987) 578; (i) G. Jaradat, K. Barqawi and T. S. Akasheh, *Inorg. Chim. Acta, 116* (1986) 63; (j) R. Ruminski and R. T. Cambron, *Inorg. Chem., 29* (1990) 1575; (k) M. B. Robin and P. Day, *Adv. Inorg. Chem. Radiochem., 10* (1967) 247.

20 (a) R. J. Watts, *Inorg. Chem., 20* (1981) 2302; (b) M. K. DeArmond and J. E. Hillis, *J. Chem. Phys., 54* (1971) 2247; (c) R. J. Watts and G. A. Crosby, *J. Am. Chem. Soc., 93* (1971) 3184.

21 J. L. Kahl, K. W. Hanck and M. K. DeArmond, *J. Phys. Chem., 82* (1978) 540.

22 (a) M. Kasha, *Discuss. Faraday Soc., 9* (1950) 14; (b) O. Buchardt, *Photochemistry of Heterocyclic Compounds,* Wiley–Interscience, New York, 1976, pp. 1–32.

23 (a) S. W. Jones, C. Franco, L. M. Vogler and K. J. Brewer, work in progress; (b) M. M. Richter, K. J. Brewer, *Inorg. Chem.,* (1993) submitted for publication; (c) L. Laverman, G. E. Jensen and K. J. Brewer, *Inorg. Chem.,* (1993) manuscript in preparation; S. M. Molnar, J. S. Bridgewater and K. J. Brewer, *J. Am. Chem. Soc.,* (1993) submitted for publication.